Identification of Load Current Influences on Position Estimation Errors for Sensorless SPMSM Drives

Hechao Wang, Kaiyuan Lu, Dong Wang, Frede Blaabjerg
Department of Energy Technology
Aalborg University
Aalborg 9220, Denmark
Email: {hec, klu, dwa, fbl}@et.aau.dk

***Abstract*—For low-speed sensorless Surface mounted Permanent Magnet Synchronous Machine (SPMSM) drives, the position is often estimated based on the rotor magnet saliency. Magnetic field distortion caused by load current may change the orientation of the rotor magnet saliency and it is therefore no longer aligned with the rotor mechanical saliency. This paper analyzes the cross-saturation effects caused by load current influence on SPMSM sensorless drives with respect to position estimation error; a new method is proposed to reliably detect the saturation dependent position estimation error that may influence the performance of sensorless SPMSM drives. Motor parameters are not required in the proposed saturation dependent position estimation error detection method and there is no need to lock the rotor. The method is suitable to use at any initial rotor position without causing noticeable rotor movement. Experimental results are presented to validate the effectiveness of the proposed methods.**

Keywords—PMSM; sensorless; cross-saturation; position error

I. INTRODUCTION

PMSM is widely used in modern industries due to its well-known advantages of high efficiency, compact size and high torque density [1]. Field Oriented Control (FOC) is often adopted for effective control of the PMSM which requires the rotor position information. Instead of using a shaft encoder, various position estimators (known as sensorless drives) have been extensively studied in the last few decades for the purposes of reducing the cost and increasing the reliability.

Sensorless control methods are normally divided into two categories for operations at medium-high speed range and at zero-low speed range, respectively [2]. For medium-high speed range operation, sensorless control methods often utilize the fundamental model of PMSM. The main idea is to detect the rotor position contained in the machine back-EMF voltage [3]. Full-order [4] or reduced-order [5] state observers may be used. This kind of methods is not suitable for zero-low speed application due to the low back-EMF voltage when the speed is low. At zero-low speed range, the rotor saliency will then be utilized for position estimation by injecting e.g. steady state high frequency signals [6, 7], or testing voltage pulses [8, 9]. For high frequency signal injection methods utilizing the steady state response, some are implemented in the stationary reference frame [6], followed by extracting the negative sequence current component by using a synchronous reference frame filter for position estimation. This method will increase current ripple on the q-axis, and consequently, the torque ripple. To overcome this disadvantage, high frequency voltage signals may be injected in the estimated d-axis [7]. However, high frequency signal injection methods implemented in stationary or synchronous reference frame need filters to, on one hand, extract the steady state high frequency current components for position estimation, and on the other hand, to suppress the high frequency signals in the current control loop in FOC. The use of filters will degrade the system dynamic performance. To have better dynamic performance, the pulse-injection-based methods are proposed, which utilize the derivative of the current information to estimate the rotor position [8, 9].

However, independent of the injection scheme chosen, only the magnetic rotor saliency, which will be influenced by saturation effects, may be detected [6-9]. The magnetic field produced by machine q-axis current may affect the saturation of the motor magnetic path, and consequently, the orientation of the rotor magnetic saliency when compared to the rotor mechanical saliency (which is also the rotor magnetic saliency at no-load). This deviation appears as position estimation error, which is difficult to be corrected by the chosen position estimation method itself [10]. To solve this problem, the relationship between the load current and saturation dependent position estimation error needs to be obtained first. There are mainly two kinds of methods to obtain this saturation dependent position estimation error. The first kind is to calculate the position estimation error using mutual inductances caused by cross-saturation effects [10-12]. This is often done by finite element analysis with machine model simulation software [10, 11], requiring the detailed knowledge of PMSM which is often not available for many industrial applications. The mutual inductances caused by cross-saturation effects may be identified by injecting special current signals to the machine [12]. But it still needs many other motor parameters for calculation of the saturation dependent position estimation error. The change of the machine parameters at different working conditions will make these machine-model based approaches more complicated to use. The other kind of methods is to measure the mechanical rotor position with extra devices, e.g. position sensor [13] and/or rotor locking devices [14]. Then the saturation dependent position estimation error could be calculated by comparing the estimated position with the measured mechanical position. However, it is obviously

difficult to implement rotor locker in many industrial applications.

In this paper, the saturation dependent position estimation error is analyzed first. Then, a new method for detecting the relationship between load current and position estimation error is proposed, with the advantages that the motor parameters are not required in the proposed methods and there is no need to lock the rotor or use a position sensor.. The obtained saturation dependent positon error is used on-line for position estimation error compensation, which validates the effectiveness of the proposed methods.

II. CONTROL FUNDAMENTALS

The voltage equations of the PMSM in the dq-reference frame are known as:

$$\begin{bmatrix} u_d \\ u_q \end{bmatrix} = R\begin{bmatrix} i_d \\ i_q \end{bmatrix} + \frac{d}{dt}\begin{bmatrix} \lambda_d \\ \lambda_q \end{bmatrix} + \omega_r \begin{bmatrix} 0 & -1 \\ 1 & 0 \end{bmatrix}\begin{bmatrix} \lambda_d \\ \lambda_q \end{bmatrix}$$
$$\begin{bmatrix} \lambda_d \\ \lambda_q \end{bmatrix} = \begin{bmatrix} L_d & 0 \\ 0 & L_q \end{bmatrix}\begin{bmatrix} i_d \\ i_q \end{bmatrix} + \lambda_{mpm}\begin{bmatrix} 1 \\ 0 \end{bmatrix} \quad (1)$$

where u_d, u_q, i_d, i_q are the stator dq-axes voltages and currents respectively; L_d, L_q are the dq-axes inductances respectively; R is the stator resistance; ω_r is rotor electrical speed; λ_d, λ_q are the dq-axes flux linkages respectively and λ_{mpm} is the peak value of the rotor PM flux linkage.

A typical sensorless drive based on FOC is shown in Fig. 1. The rotor position information is essential for transformations in the FOC system. For sensorless control, the rotor position is estimated by using electrical signals instead of being provided from position sensors. In sensorless algorithms, motor terminal voltages, currents and motor parameters may be involved in the position estimation. In this paper, to avoid the uncertainties in motor terminal voltages and motor parameters, only motor phase currents are used for estimating the rotor position.

III. SENSORLESS ALGORITHM

In Pulse Width Modulation (PWM) controlled Voltage Source Inverter (VSI), the nonlinear switch characteristics may distort the VSI output voltage. Thus the inverter nonlinear characteristics need to be introduced in the machine equations. Then (1) becomes:

$$\begin{bmatrix} u_d^* \\ u_q^* \end{bmatrix} = R\begin{bmatrix} i_d \\ i_q \end{bmatrix} + \frac{d}{dt}\begin{bmatrix} \lambda_d \\ \lambda_q \end{bmatrix} + \omega_r \begin{bmatrix} 0 & -1 \\ 1 & 0 \end{bmatrix}\begin{bmatrix} \lambda_d \\ \lambda_q \end{bmatrix} + \begin{bmatrix} u_{d\_inverter} \\ u_{q\_inverter} \end{bmatrix} \quad (2)$$

where u_d^*, u_q^* are dq-axes voltage reference values generated by current controllers in FOC and $u_{d\_inverter}$, $u_{q\_inverter}$ are dq-axes inverter voltage errors respectively.

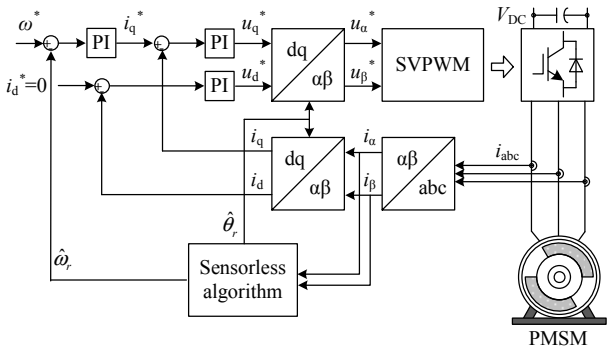

Fig. 1. Sendorless FOC system for SPMSM.

Almost all pulse-injection-based sensorless algorithms are tracking inductance-based saliency. However the cross-saturation effects may affect the motor inductance and introduce position estimation error. Thus the cross-saturation effects need to be taken into account and then dq-axes flux linkages become,

$$\begin{bmatrix} \lambda_{ds} \\ \lambda_{qs} \end{bmatrix} = \begin{bmatrix} L_d & L_{dq} \\ L_{qd} & L_q \end{bmatrix}\begin{bmatrix} i_d \\ i_q \end{bmatrix} + \lambda_{mpm}\begin{bmatrix} 1 \\ 0 \end{bmatrix} \quad (3)$$

where L_{dq} and L_{qd} are the mutual inductances caused by cross-saturation effects and the subscript s in the flux linkages denotes cross-saturation effects. It is often assumed that the cross-coupling effects from the d-axis to the q-axis is identical to that from the q-axis to the d-axis, i.e. L_{dq} is made equal to L_{qd}.

Assuming that the resistance voltage drop, speed dependent voltage drop and inverter voltage error do not change during two neighbouring switching periods, the two voltage equations in these two neighbouring switching periods may be given as

$$\begin{bmatrix} u_{d1}^* \\ u_{q1}^* \end{bmatrix} = R\begin{bmatrix} i_d \\ i_q \end{bmatrix} + \frac{d}{dt}\begin{bmatrix} \lambda_{ds1} \\ \lambda_{qs1} \end{bmatrix} + \omega_r \begin{bmatrix} 0 & -1 \\ 1 & 0 \end{bmatrix}\begin{bmatrix} \lambda_{ds} \\ \lambda_{qs} \end{bmatrix} + \begin{bmatrix} u_{d\_inverter} \\ u_{q\_inverter} \end{bmatrix}$$
$$\begin{bmatrix} u_{d2}^* \\ u_{q2}^* \end{bmatrix} = R\begin{bmatrix} i_d \\ i_q \end{bmatrix} + \frac{d}{dt}\begin{bmatrix} \lambda_{ds2} \\ \lambda_{qs2} \end{bmatrix} + \omega_r \begin{bmatrix} 0 & -1 \\ 1 & 0 \end{bmatrix}\begin{bmatrix} \lambda_{ds} \\ \lambda_{qs} \end{bmatrix} + \begin{bmatrix} u_{d\_inverter} \\ u_{q\_inverter} \end{bmatrix} \quad (4)$$

where the subscripts 1 and 2 denote the first and second switching period respectively. By subtraction of the first switching period voltage equation from the second switching period voltage equation, the voltage equation may be greatly simplified to.

$$\begin{bmatrix} \Delta u_d \\ \Delta u_q \end{bmatrix} \approx \begin{bmatrix} L_d & L_{dq} \\ L_{dq} & L_q \end{bmatrix}\frac{d}{dt}\begin{bmatrix} \Delta i_d \\ \Delta i_q \end{bmatrix} \quad (5)$$

where subscript Δ represents the difference between the two neighbouring switching periods. In (5), the influences of

uncertain voltage components such as the inverter voltage error, phase resistive voltage drop and back-EMF voltage components are removed. To estimate the rotor position, (5) is preferred to be transformed into the estimated dq-reference frame, as:

$$\begin{bmatrix}\Delta u_{\hat{d}}\\ \Delta u_{\hat{q}}\end{bmatrix}=\begin{bmatrix}L_0+L_1\cos 2(\tilde{\theta}_r+\varepsilon) & L_1\sin 2(\tilde{\theta}_r+\varepsilon)\\ L_1\sin 2(\tilde{\theta}_r+\varepsilon) & L_0-L_1\cos 2(\tilde{\theta}_r+\varepsilon)\end{bmatrix}\frac{d}{dt}\begin{bmatrix}\Delta i_{\hat{d}}\\ \Delta i_{\hat{q}}\end{bmatrix} \quad (6)$$

where $\varepsilon = 0.5\cdot\arctan 2L_{dq}/(L_d - L_q)$ and it is the saturation dependent position estimation error since when L_{dq} is zero, ε is zero; $\tilde{\theta}_r$ is the position error between the estimated d-axis and the real machine d-axis and $L_0 = (L_d + L_q)/2$, $L_1 = \sqrt{[(L_d - L_q)/2]^2 + L_{dq}^2}$. If choosing the voltage vectors applied in the two neighbouring switching periods in (5) to be opposite to each other and both are aligned with the estimated d-axis, the following equation could be obtained.

$$\frac{\Delta(\Delta i_{\hat{q}})}{T_s}\approx\frac{d\Delta i_{\hat{q}}}{dt}=\frac{-L_1\Delta u_{\hat{d}}}{L_0^2-L_1^2}\sin(2\tilde{\theta}_r+2\varepsilon) \quad (7)$$

where T_s is the switching period. In one switching period, the differential $d\Delta i_{\hat{q}}/dt$ may be approximated by $\Delta(\Delta i_{\hat{q}})/T_s$.

The implementation of the described voltage vector injection scheme combined with FOC voltage output is shown in Fig. 2. The current at the beginning of each switching period is measured. The current difference is used for position error estimation as (7). Then the estimated rotor position and the estimated rotor speed could be obtained by passing the estimated position error (7) to a classical PLL controller as shown in Fig. 3 [15]. No filter is needed for extracting the high frequency current signal and it does not affect the fundamental current component used in FOC. It is worth to point out here that the PLL estimates the position by forcing the input estimated position error (7) to be zero. Ideally, when there are no cross-saturation effects, the estimated position corresponds to $\tilde{\theta}_r = 0$. With L_{dq} present, the estimated position corresponds to $\tilde{\theta}_r + \varepsilon = 0$, generating an error term of ε, which is cross-saturation level dependent. L_{dq} is zero at no load. When the q-axis current increases, ε increases.

IV. Saturation Dependent Position Estimation Error Detection

The saturation dependent position estimation error ε introduced by the q-axis current cannot be corrected by the position estimation algorithm itself [6]. Additional methods have to be used to identify this error and to compensate it afterwards.

It is preferred that before running the machine with a chosen sensorless algorithm, the value of ε with respect to different q-axis current i_q should be estimated first. The obtained information may then be conveniently used to correct the estimated position used for the sensorless operation of the drive.

A. Initial Position Detection

To obtain the relationship between ε and i_q, there are mainly 3 elements required, θ_r, $\hat{\theta}_r$ and i_q. Due to there is no position sensor in the sensorless drive system, θ_r (the mechanical rotor position) is difficult to be measured. Thus an initial positon estimation method is employed here with no q-axis current present and the estimated initial position is regarded as θ_r [16].

B. Determination of Detection Period

Another difficulty in detecting the saturation dependent position estimation error is that when keeping a desired q-axis current, the machine is actually in torque control mode; if the generated torque is higher than the load torque, the machine will keep accelerating. For an electrical machine drive system, the mechanical time constant is often much larger than the electrical time constant. So if the detection algorithm with i_q present could be conducted in a very short time (only few switching periods), then the machine rotor will only have a very small rotation and is regarded as standstill. This short time t could be calculated by PMSM torque equation as shown below:

$$\begin{aligned} J\frac{d\omega}{dt} &= \frac{3}{2}p[\lambda_{mpm}i_q + (L_d - L_q)i_d i_q] - T_L\\ \omega &= \frac{d\theta_r}{dt}\frac{1}{p}\end{aligned} \quad (8)$$

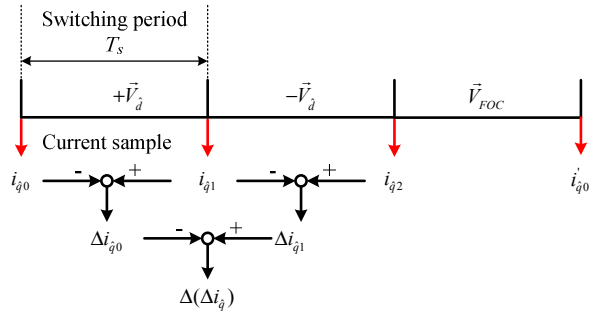

Fig. 2. Implementation of Sendorless Method

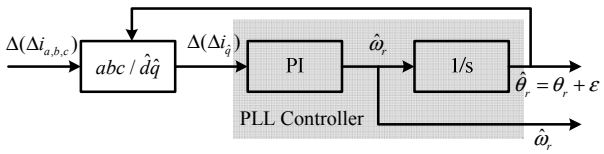

Fig. 3. PLL Controller for Sensorless Metho

where ω is rotor mechanical speed; J is the drive system inertia; p is pole pairs; T_L is the load torque. It should be noted that the angular acceleration obtained from (8) is over-estimated since the friction is ignored. For real conditions where friction exists, smaller rotation angle will exhibit. In the proposed method for SPMSM, d-axis current reference is set to be zero. Assuming the load torque is zero, the time before the rotor has rotated an angle more than $\theta_{\min}$ could be obtained by:

$$t = \sqrt{\frac{4}{3}\frac{J\theta_{\min}}{p^2\lambda_{mpm}i_q}} \tag{9}$$

where $\theta_{\min}$ is the minimum angle of the rotor may rotate before losing its standstill condition and t is the time for the rotational angle to reach $\theta_{\min}$. The experimental verification is shown in section V.

C. Choosing Suitable Position Estimation Method

Due to the fact that there is only a few switching periods available for detecting the saturation dependent position estimation error ε, the detection method must be fast enough. Therefore, pulse injection methods are employed. Since the q-axis currents must be kept constant when detecting ε, pulse injection methods in the $\alpha\beta$-reference frame such as INFORM method [2] are not suitable for such application. Fig. 4 illustrates the injected voltage vector used for the INFORM method. It can be seen that no matter what the rotor position is, there are more than one injected voltage vector containing large q-axis components, giving difficulties in maintaining a desired q-axis current value. Therefore, a pulse-injection method with minimal q-axis current influence should be employed, such as the method described by (7). It injects voltage pulse on the estimated d-axis (Fig. 4) and will not cause large q-axis current variation while the position is well estimated.

For sensorless control, a PLL is usually used to obtain the estimated position from the estimated position error. It can be seen from (7) that the machine parameters and injected voltage differences are involved. However, it should be noticed that they only influence the gain factor in (7). When the estimated position error is zero, the expected current variation on the estimated q-axis is zero, and there is no need to know the exact gain value (i.e. the term before $\sin(2\tilde{\theta}_r + 2\varepsilon)$) in (7). This means that this method can be made machine parameter and injection voltage independent. To utilize this principle in detecting ε, the estimated d-axis position (where the voltage pulse is injected) is changed for searching for a position where the current variation on the corresponding q-axis (which is 90 electrical degrees away) is minimized (i.e. $\sin(2\tilde{\theta}_r + 2\varepsilon) = 0$). Then, the estimated d-axis is aligned with the real magnetic saliency including the cross-saturation effects and $\varepsilon = -\tilde{\theta}_r$ is obtained.

This is principally illustrated in Fig. 4 and its implementation in real-time is shown in Fig. 5. According to (7), when $\Delta(\Delta i_{\hat{q}})$ is greater than zero, the estimated d-axis is leading the real d-axis and when $\Delta(\Delta i_{\hat{q}})$ is smaller than zero, the estimated d-axis is lagging the real d-axis. This gives indications on how the estimated d-axis should be corrected in order to be finally aligned with the real d-axis and under this condition, voltage injected on the estimated d-axis causes no current variation that can be detected on the corresponding q-axis.

D. Saturation Dependent Position Error Compensation

By using the detection method stated above, the saturation dependent position estimation error at different i_q values can be obtained and the obtained curve is shown in Fig. 6. Similar results could be obtained at different initial positions as e.g. shown in Fig. 6 for tests carried out at 0 and 120 electrical degrees respectively, which agree well with each other. So if the rotor cannot be rotated at a given operation condition, the curve obtained at the current initial position is enough and there is no need to rotate the rotor and repeat the test. The obtained position error versus q-axis current relationship may be implemented as a simple look-up table and may then be used to correct the position estimated by the chosen algorithm, as illustrated in Fig. 7.

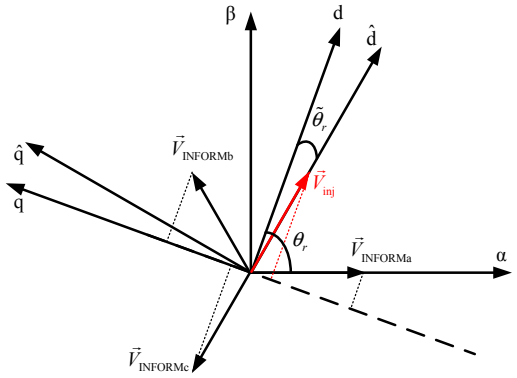

Fig. 4. Comparison of different injection methods

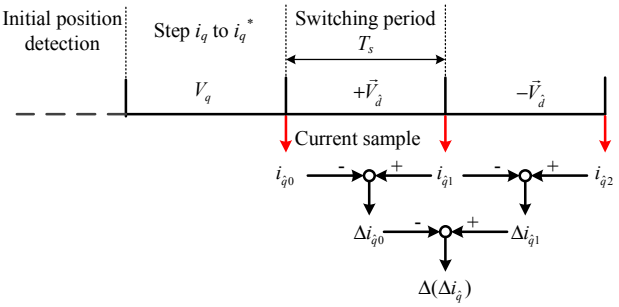

Fig. 5. Implementation of Position Error Detection

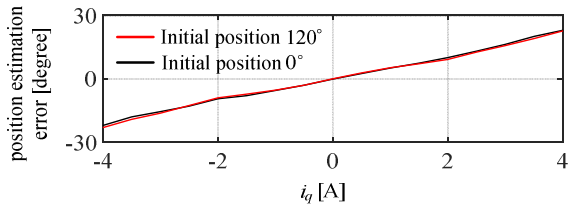

Fig. 6. Relationship Between q-axis Current and Rotor Position Error Caused by Cross-Saturation Effect at Different Initial Positions.

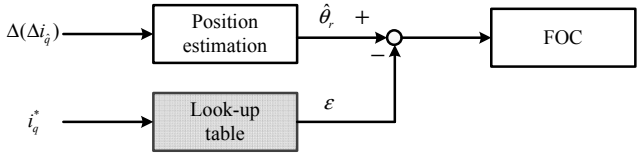

Fig. 7. Block Diagram of Position Error Compensation.

V. Experiment Results

The experiment platform is built with a PMSM, a DC motor providing load torque, a Digital Signal Processor (DSP-F28335) based controller and a Danfoss FC302 inverter. A 2048-line encoder is employed to obtain the mechanical position and speed of the PMSM for comparison. The switching frequency is set to be 5k Hz. The parameters of PMSM are listed in Table I.

A. Determination of Detection Period

To verify the principle in section IV.B, an experiment is carried out with a 4A q-axis current; the rotor rotates for 1 electrical degree after about 0.006 seconds, which means that if $\theta_{\min}$ is chosen to be 1 electrical degree, the detection algorithm is allowed to use about 30 switching periods for calculation. Comparing with the result from (9), which is about 18 switching periods, the experiment allows longer time for the detection of ε. This is due to the system friction as discussed above.

TABLE I. Parameters of PMSM

Parameters of PMSM	
Rated power [W]	400
Max. phase voltage [V]	380
Rated current [A]	2.9
Rated speed [rpm]	2850
Rated frequency [Hz]	95
Stator resistance [Ω]	2.3
d-axis inductance [mH]	10
q-axis inductance [mH]	13
PM flux linkage [Wb]	0.12
Pole pairs	2
System inertia [kg·m^2]	1e-3

The fast rise of the q-axis current as shown in Fig. 8 could be achieved by applying a proper voltage command obtained based on the machine time constant and desired reference q-axis current value, like model-predictive control. This enables the q-axis current to step up to the reference value in only one switching period. It is worth to notice that there is no need to know the exact values of motor parameters, because the aim here is to obtain the relationship between ε and i_q. Even though inaccurate motor parameters may result in that the actual q-axis current after one switching period is not close to the reference value, this measurement point can still contribute to form the ε vs. i_q curve.

B. Compearison with the Uncompensation Method at Different Load Conditions

In the experiments of this part, the real rotor speed is used in FOC and the position is from the estimation algorithm. The first experiment is to compare the drive performance without (Fig.9) and with(Fig.10) the saturation dependent position estimation error compensation under the operation condition of 50% load torque step at 15 rpm. It may be observed from Fig. 9 that the sensorless system can well handle the half-load torque step change condition even without position estimation error compensation. But due to the -12.8 degree position estimation error, the estimated q-axis current (2.06A in Fig. 9) is a little higher than that with compensation (1.98A in Fig.10), which means that for the same load torque the system without compensation method needs to draw more current. The position estimation error compensation method may help the system approach the maximum torque per ampere control.

Then a full load step is applied to the sensorless drive. As can be seen in Fig. 11, the sensorless drive is not able to handle the full load step change when without the position estimation error compensation method. However the sensorless drive can perform well at full load step change when the position estimation error compensation method is involved, as shown in Fig. 12. Meanwhile it is observed in Fig. 13 that, after a full-load torque step, the position estimation error is only 2.2 degree with the saturation dependent position estimation error compensation, which means the proposed detection method is precise.

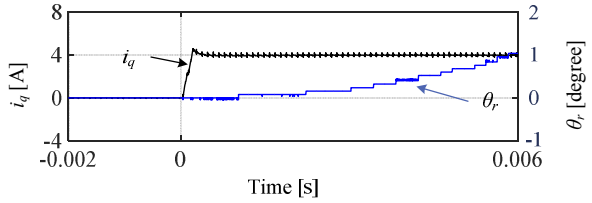

Fig. 8. q-axis Current and Rotor Position

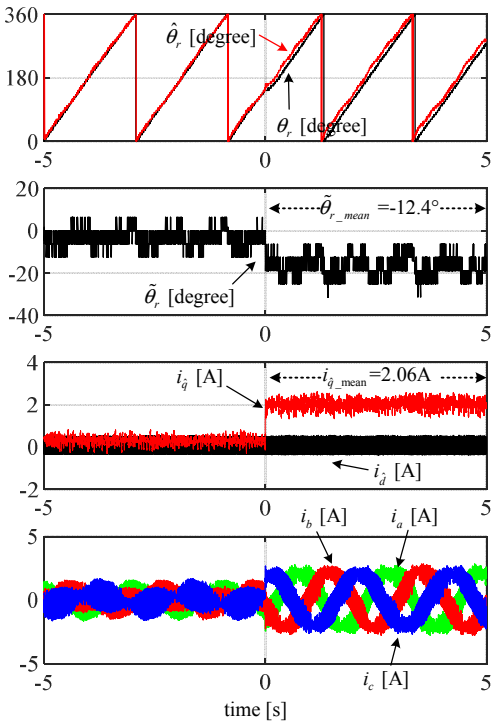

Fig. 9. 50% load torque step at 15 rpm without position error compensation. From top to bottom: real and estimated rotor position, the position error, estimated dq-reference current and 3-phase currents.

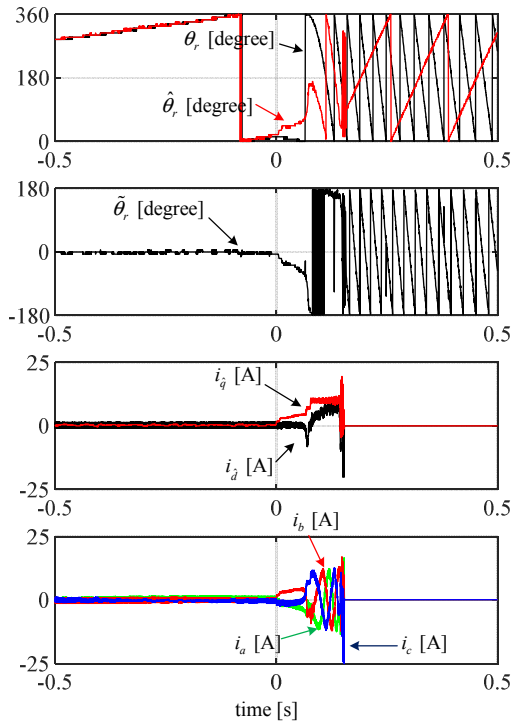

Fig. 11. 100% load torque step at 15 rpm without position error compensation. From top to bottom: real and estimated rotor position, the position error, estimated dq-reference current and 3-phase currents.

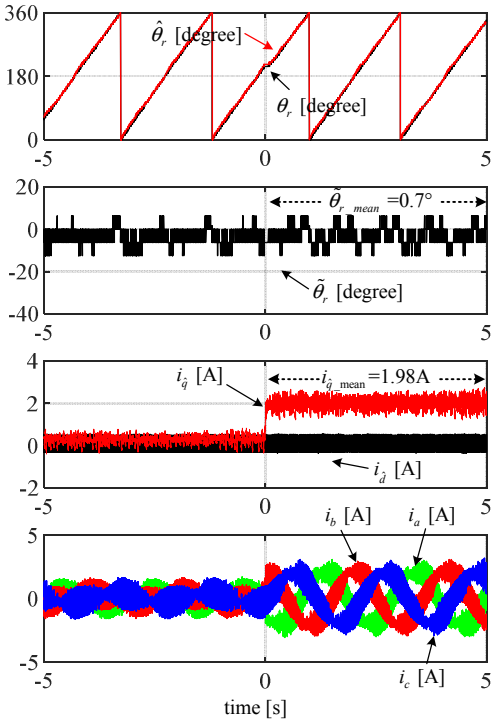

Fig. 10. 50% load torque step at 15 rpm with position error compensation. From top to bottom: real and estimated rotor position, the position error, estimated dq-reference current and 3-phase currents.

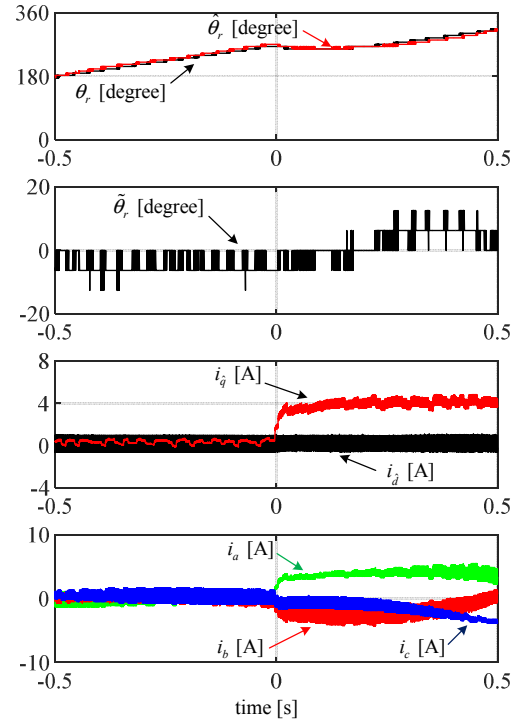

Fig. 12. 100% load torque step at 15 rpm with position error compensation. From top to bottom: real and estimated rotor position, the position error, estimated dq-reference current and 3-phase currents.

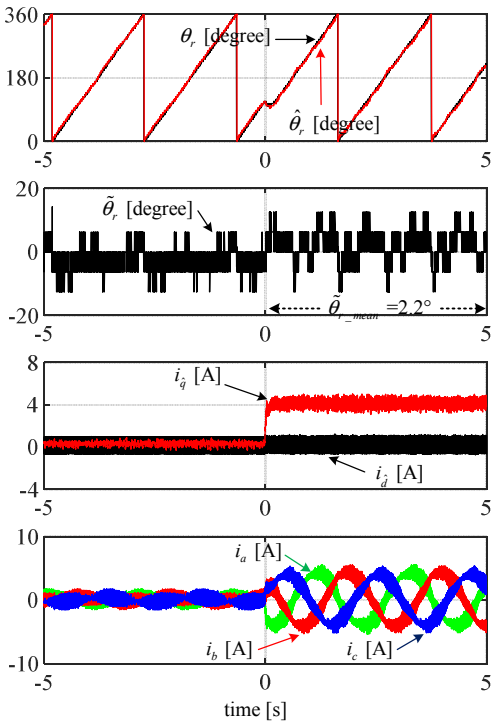

Fig. 13. Steady state performance of 100% load torque step at 15 rpm with position error compensation. From top to bottom: real and estimated rotor position, the position error, estimated dq-reference current and 3-phase currents.

VI. Conclusion

This paper analyzes the influence of the cross-saturation effect on position estimation error for a SPMSM sensorless drive system. A simple and effective method for identifying such position error without the assistance of extra devices or setup modifications is presented. The accuracy of the proposed method is verified experimentally by compensating the obtained position errors in a sensorless drive. Satisfactory results are obtained validating its effectiveness. The robustness of the sensorless drive is enhanced with the identified saturation dependent position estimation error compensated. Meanwhile the current shows a trend to be reduced with the identified saturation dependent position estimation error compensated.

References

[1] P. P. Acarnley and J. F. Watson "Review of position-sensorless operation of brushless permanent-magnet machines," *IEEE Trans. on Ind. Electron.*, vol. 53, no. 2, pp. 352-362, 2006.

[2] Y. Zhao, C. Wei, Z. Zhang, and W. Qiao, "A Review on Position/Speed Sensorless Control for Permanent-Magnet Synchronous Machine-Based Wind Energy Conversion Systems," *IEEE J.Emerg. Sel. Topics Power Electron.*, vol. 1, no. 4, pp. 203-216, 2013.

[3] I. Boldea, M. C. Paicu, and G. D. Andreescu, "Active Flux Concept for Motion-Sensorless Unified AC Drives," *IEEE Trans. Power Electron.*, vol. 23, no. 5, pp. 2612-2618, 2008.

[4] J. Solsona, M. I. Valla, and C. Muravchik, "Nonlinear control of a permanent magnet synchronous motor with disturbance torque estimation," *IEEE Trans. Energy Convers.*, vol. 15, no. 2, pp. 163–168, 2000.

[5] J. S. Kim, S. L. Sul, "High Performance PMSM Drives without Rotational Position Sensors Using Reduced Order Observer," *IEEE Thirtieth IAS Annual Meeting Conference on Industry Applications,* vol. 1, pp. 75-82, 1995.

[6] M. W. Degner, R. D. Lorenz, "Using Multiple Saliencies for the Estimation of Flux, Position, and Velocity in AC Machines," *IEEE Trans. Ind. Appl*, vol. 34, no. 5, pp. 1097-1104, 1998.

[7] M. J. Corley, R. D. Lorenz, "Rotor Position and Velocity Estimation for a Salient-Pole Permanent Magnet Synchronous Machine at Standstill and High Speeds," *IEEE Trans. Ind. Appl*, vol. 34, no. 4, pp. 784-789, 1998.

[8] M. Schroedl, "Sensorless Control of AC Machines at Low Speed and Standstill Based on the "INFORM" Method," *IEEE IAS Annual Meeting,* pp. 270-277, Oct 1996.

[9] G. Xie, K. Lu, S. K. Dwivedi, J. R. Rosholm and F. Blaabjeg. "Minimum Voltage Vector Injection Method for Sensorless Control of PMSM for Low-Speed Operations," *IEEE Trans.Power Electron.*, vol. 31, no. 2, pp. 1785-1794, 2016.

[10] J. M. Liu, Z. Q. Zhu. "Novel Sensorless Control Strategy with Injection of High-Frequency Pulsating Carrier Signal into Stationary Reference Frame," *IEEE Tran Ind Appl*. vol. 50, no. 4, pp. 2574-2583, 2014.

[11] Z. Q. Zhu, Y. Li, D. Howe, C. M. Bingham. "Compensation for Rotor Position Estimation Error due to Cross-Coupling Magnetic Saturation in Signal Injection Based Sensorless Control of PM Brushless AC Motors," *Proc.IEEE Electric Machines & Drives Conf.*, pp.208-213, 2007.

[12] S. Ebersberger, B. Piepenbreier "Identification of Differential Inductances of Permancet Magnet Synchronous Machines Using Test Current Signal Injection," *Proc. Symp. Power Electronics, Electrical Drives, Automation and Motion*, pp. 1342-1347, 2012.

[13] H. W. De Kock, M. J. Kamper, R. M. Kennel. "Anisotropy Comparison of Reluctance and PM Synchronous Machines for Position Sensorless Control Using HF Carrier Injection," *IEEE Trans on Power Electron*, vol. 24, no. 8, 2009.

[14] N. Teske, G. M. Asher, M. Sumner. K.J Bradley. "Suppression of saturation saliency effects for the sensorless position control of induction motor drives under loaded conditions," *IEEE Trans on Ind Electron*. vol. 47, no. 5, 2000.

[15] J. L. Chen, T. H. Liu, C. L. Chen, "Design and implementation of a novel high-performance sensorless control system for interior permanent magnet synchronous motors," *IET Electric Power Appl.*, vol. 4, no. 4, pp. 226-240, 2010.

[16] M. Boussak, "Implementation and experimental investigation of sensorless speed control with initial rotor position estimation for interior permanent magnet synchronous motor drive," *IEEE Trans on Power Electron*, vol. 20, no. 6, 2005.